Numerical simulation of the sound pressure level distributions at the entrance of individual external ears

Nele Hauenschild[1,2], Reinhild Roden[2], Matthias Blau[2,3]
[1] *Medizinische Physik, Carl von Ossietzky Universität Oldenburg, Germany.*
[2] *Institut für Hörtechnik und Audiologie, Jade-Hochschule, Oldenburg, Germany.*
[3] *Cluster of Excellence "Hearing4All".*
Email: matthias.blau@jade-hs.de

Abstract
Aiming at individualized acoustic transparency for users of in-ear hearing systems, we investigate to which extent it is possible to estimate open-ear sound transfer from measurements taken while wearing an in-ear hearing system that is blocking the ear canal. One of the prerequisites for an ideal estimation of the open-ear characteristics is that the sound field within the ear canal be one-dimensional (along a curved axis). This is a valid assumption at low frequencies and positions away from the concha, ear canal bends and the eardrum, but may be questionable at typical earpiece faceplate locations. In this work, we investigate the distribution of sound pressure levels across a surface on the faceplate of an earpiece with and without vent, compared to an open ear canal, for different angles of sound incidence. First results of 3D BEM simulations for three individual head geometries of the IHA database indicate that for the frequency range up to about 4 kHz the sound pressure level distribution on the faceplate surface is sufficiently uniform, such that a one-dimensional approach to construct individualized transparency filters appears to be feasible.

Introduction
To improve the sound quality of in-ear hearing systems, individualized equalization algorithms are being researched, with the goal to provide acoustic transparency. This means that the natural hearing perception with open ears should be restored when wearing the in-ear device. In previous work, the focus was mainly on the prediction of the sound pressure at the individual eardrum in the aided ear by using one-dimensional electro-acoustic models [1], [2], [3], [4], [5]. These methods were successful since the prerequisite of a one-dimensional wave propagation in the ear canal was met at the considered locations in the main frequency range of up to 10 kHz. However, to achieve individualized transparency, the outer sound field (which is three-dimensional) must be captured in a person-specific way at a position from where on a one-dimensional (direction-independent) transfer can be assumed. The usual assumption is that this position is located at the entrance to the blocked ear canal [6]. However, in-the-ear devices may deviate from a typical blocked-ear scenario, such as that used in HRTF measurements, in that they may (a) protrude out of the ear and (b) contain vent openings.

The present study aims to assess the extent to which the prerequisites for coupling the outer 3D sound field to the one-dimensional model are satisfied for a typical vented in-ear hearing system in realistic human ears. To this end, numerical simulations are used to analyze the sound pressure distribution at the entrance of the open individual ear and on the faceplate of the hearing system, respectively.

Methods
a) Geometry models
The IHA database, which comprises three-dimensional models of the torso, head, and complete outer ears with ear canals and eardrums, is under development and partly published [7]. The methodology employed in the creation of these geometries has been previously described [8]. The present study involves the use of geometry models of the right ear canals from subjects 1, 2 and 3 of the database.
The models were supplemented with a simplified individual ear mold wrapping the prototype of an in-ear hearing device that is currently being developed. Figure 1 illustrates both the aided (i.e., with the hearing system inserted) and the unaided (i.e., open ear) cases. The hearing device features a vent opening (rightmost circle on the faceplate). The current prototype of this hearing system is equipped with two microphones on the faceplate (indicated by the two other circles on the faceplate), capable of collecting direction-dependent information from the external sound field.

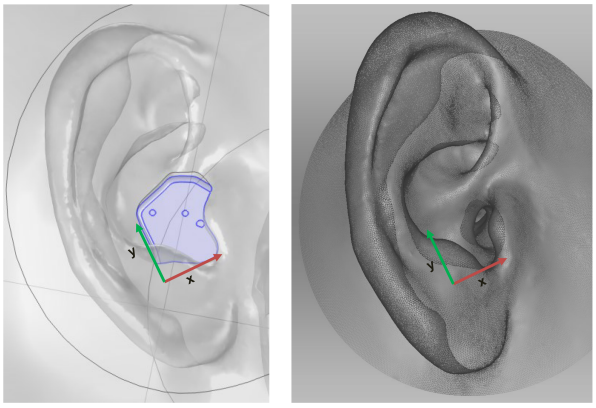

Figure 1: Exemplary individual outer ear geometry of one participant: blocked with the earpiece inserted into the ear (left) and open ear canal (right).

b) 3D BEM simulations

3D BEM simulations were performed using COMSOL Multiphysics 6.2 (COMSOL AB, Stockholm, Sweden) with the the three individual head geometries (without torso) discussed above. Four external sources were placed in the horizontal plane at the front and back, as well as at the ipsilateral and contralateral sides, in a distance of 1.5 m from the inter-aural center. The simulations were repeated for ***three conditions***: ***a)*** *Inserted Earpiece with vent,* ***b)*** *Inserted Earpiece without/sealed vent,* ***c)*** *Open ear without hearing device.*

For condition a), the input impedance of the vent terminated by the residual ear canal of each individual geometry was first computed via a 3D FEM simulation (again, using COMSOL). This pre-computed input impedance was then assigned as a boundary condition to the vent input surface in the BEM model. Fig. 2 shows one exemplary geometry of the vent with the coupled residual ear canal as used in the 3D FEM simulation.

From the BEM simulations, the sound pressure $p(\vartheta, \varphi, x, y)$ was extracted on a grid of points on the evaluation surface (plane on the faceplate of the hearing device, with x and y giving the main axes of the plane as illustrated in Fig. 2), and the spherical coordinates φ and ϑ giving the direction of sound incidence.

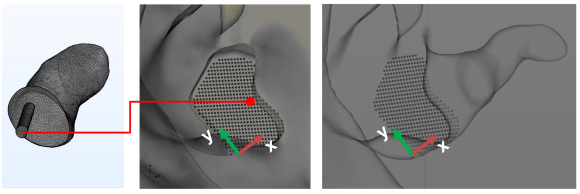

Figure 2: Example of outer ear with evaluation points: Mesh of the vent terminated by the residual ear canal for the pre-calculation of the vent input impedance (left), evaluation points on the faceplate of the inserted earpiece (middle), and the same evaluation points in the open ear canal condition (right).

The sound pressure level distributions on the evaluation surface were then evaluated in two different ways, namely a) location-based and b) frequency-dependent. For the location-based analysis, the absolute sound pressure levels at specific frequencies of interest were interpolated over all evaluation points and shown on a surface plot that recreates the surface of the earpiece. In the frequency-dependent analysis, 5th and 95th percentiles of the level differences (between sound pressure levels at the evaluation points and the level at the reference point shown in fig. 3) on a subset of the evaluation points were computed and shown as a function of frequency. The subset was defined such that all evaluation points, except in the outer rim and vent regions where microphone positions would not be feasible, were included, see fig. 3.

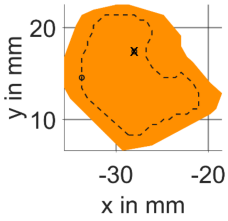

Figure 3: Region of evaluation (inside dashed line) and reference point (x) on the faceplate.

Results

a) Location-based analysis of the sound pressure level distribution on the evaluation surface

The sound pressure level distribution on the evaluation surfaces, extracted from the simulation of subject 1, is shown in Fig. 4 at selected frequencies and for all four source directions.

At 500 Hz, the sound pressure level distribution is uniform, regardless of condition and direction of incidence. As expected, the level is moderately higher for the ipsilateral source in comparison to the other directions of incidence. At 5000 Hz, the sound pressure level distribution is still close to uniform, except on the vent surface in condition a) and in the tragus region for the contralateral source. The absolute levels now depend much more on the direction of incidence, without surprises (i.e., largest for the ipsilateral source, smallest for the contralateral source, and somewhere inbetween for the frontal and back sources). Apart from in the immediate vicinity of the vent opening, all three conditions (vented earpiece, blocked earpiece, open ear) behave much in the same way. At even higher frequencies, the level distributions vary considerably, both as a function of condition and of the direction of incidence. Similar observations were made for the other two subjects (not shown here).

b) Frequency-dependent analysis of the sound pressure level distribution on the evaluation surface

The results of the frequency-dependent analysis are shown in fig. 5.

One can distinguish three frequency regions: At low frequencies up to about 4 kHz there is no or almost no variation in the level distribution, regardless of condition and direction of incidence. At frequencies between 4 kHz and 7 kHz, the amount of variability depends on the direction of incidence: it is highest for contralateral incidence, followed by frontal and rear and ipsilateral sound incidence. At high frequencies above 7 kHz a high variability is observed for all conditions and directions of incidence. Again, similar observations were made for the other participants (not shown here).

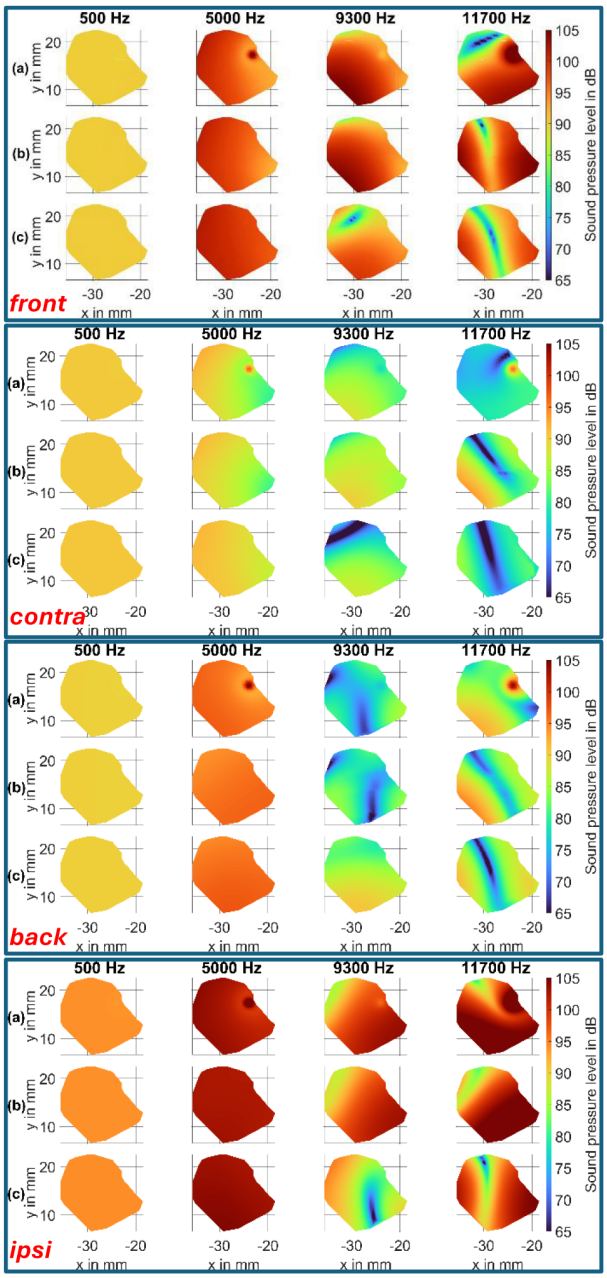

Figure 4: Sound pressure level distribution on the evaluation surfaces, extracted from the simulation of subject 1, at selected frequencies (columns) and all angles of sound incidence (from top to bottom). a) vented earpiece, b) closed earpiece, and c) open ear.

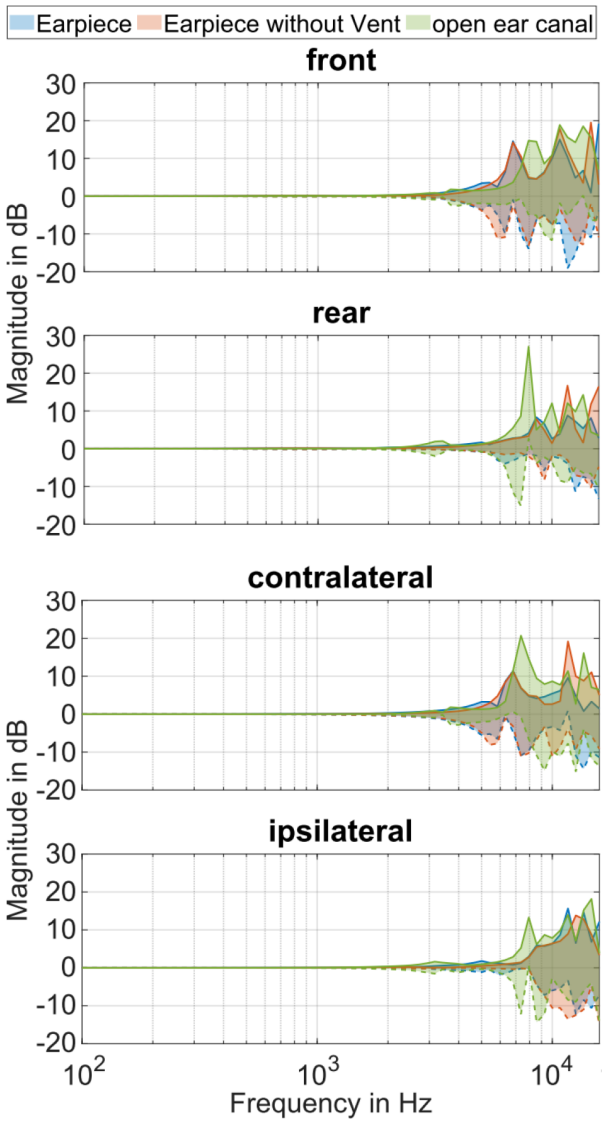

Figure 5: Frequency-dependent distribution of sound pressure level differences with respect to the reference point shown in fig. 3: 5th and 95th percentiles of all points on the surface shown in fig. 3 as well, for subject 1.

Summary and Discussion

In summary, up to 4 kHz, the sound pressure level distribution on a plane at the entrance of three human ear canals is uniform with a maximum deviation of 5 dB from the reference point. At mid-frequencies between 4 and 7 kHz, there is still a uniform appearance with rear and ipsilateral sound incidence, but moderate deviations with frontal and contralateral sound incidence. Above 7 kHz, vertical and horizontal patterns appear in the sound pressure distribution, partially influenced by the vent. However, there are still narrow frequency bands with nearly uniform distributions between 7 and 12 kHz.

To interpret the results, the methods used must be taken into account. There are high, sudden deviations in the level distribution, as shown in the percentile view in Fig. 5, due to a rather low frequency resolution (30 frequency points per decade). In addition, there are different surface angles with respect to the entrance plane of the ear canal and different surface sizes between subjects. This limits the comparability between the three subjects used for the simulations. The shape of the faceplate is simplified with an idealized fitting and sealing of the ear. Unlike in real life, there is no repetition of the insertion of the earpiece into the ear.

Conclusion

The sound pressure level distribution at the entrance of the ear canal with an in-ear hearing system inserted can be assumed to be uniform up to 4 to 5 kHz. The presence of a vent can be neglected when microphones are used at reasonable positions on the faceplate of the in-ear device. These results indicate that individualized transparency algorithms are feasible in the speech frequency range.

Acknowledgments

This research was partially funded by the Deutsche Forschungsgemeinschaft (DFG, German Research Foundation)—Project ID 352015383—SFB 1330 C1.

References

[1] Blau, M., Sankowsky, T., Roeske, P., Mojallal, H., Teschner, M., and Thiele, C. (2010). “Prediction of the sound pressure at the ear drum in occluded human cadaver ears,” Acta Acustica united with Acustica 96(3), 554–566.

[2] Sankowsky-Rothe, T., Blau, M., Mojallal, H., Teschner, M., and Thiele, C. (2012). “Prediction of the sound pressure at the ear drum for open fittings,” in Acoustics 2012.

[3] Sankowsky-Rothe, T., Blau, M., Köhler, S., and Stirnemann, A. (2015). “Individual equalization of hearing aids with integrated ear canal microphones,” Acta Acustica united with Acustica 101(3), 552–566.

[4] Vogl, S., and Blau, M. (2019). “Individualized prediction of the sound pressure at the eardrum for an earpiece with integrated receivers and microphones,” The Journal of the Acoustical Soci- ety of America 145(2), 917–930.

[5] Wulbusch, N., Roden, R., Chernov, A., and Blau, M. (2023). “Us- ing a one-dimensional finite-element approximation of webster’s horn equation to estimate individual ear canal acoustic transfer from input impedances,” The Journal of the Acoustical Society of America 153(5), 2826–2826.

[6] Hammershøi, D., Møller, H. (1996). Sound transmission to and within the human ear canal. Journal of the Acoustical Society of America, 100(1), 408-427.

[7] Roden, R., and Blau, M. (2021). “The iha database of human geometries including torso, head and complete outer ears for acoustic research”, https://doi.org/10.5281/zenodo.5528765, doi: 10.5281/zenodo.5528765 .

[8] Roden, R., and Blau, M. (2020). “The iha database of human ge- ometries including torso, head and complete outer ears for acous- tic research,” in INTER-NOISE and NOISE-CON Congress and Conference Proceedings, Institute of Noise Control Engineering, Vol. 261, pp. 4226–4237.